

## Accepted Manuscript

Title: Activity/selectivity control in Pd/H<sub>x</sub>MoO<sub>3</sub> catalyzed cinnamaldehyde hydrogenation

Author: M. Kołodziej A. Drelinkiewicz E. Lalik J. Gurgul D. Duraczyńska R. Kosydar



PII: S0926-860X(16)30028-X  
DOI: <http://dx.doi.org/doi:10.1016/j.apcata.2016.01.028>  
Reference: APCATA 15743

To appear in: *Applied Catalysis A: General*

Received date: 9-11-2015  
Revised date: 21-1-2016  
Accepted date: 22-1-2016

Please cite this article as: M.Kołodziej, A.Drelinkiewicz, E.Lalik, J.Gurgul, D.Duraczyńska, R.Kosydar, Activity/selectivity control in Pd/H<sub>x</sub>MoO<sub>3</sub> catalyzed cinnamaldehyde hydrogenation, Applied Catalysis A, General <http://dx.doi.org/10.1016/j.apcata.2016.01.028>

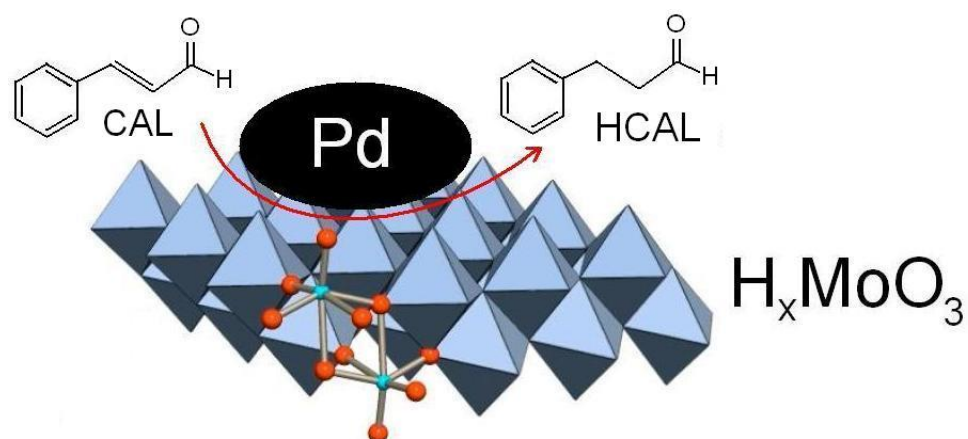
This is a PDF file of an unedited manuscript that has been accepted for publication. As a service to our customers we are providing this early version of the manuscript. The manuscript will undergo copyediting, typesetting, and review of the resulting proof before it is published in its final form. Please note that during the production process errors may be discovered which could affect the content, and all legal disclaimers that apply to the journal pertain.

Activity / selectivity control in Pd/H<sub>x</sub>MoO<sub>3</sub> catalyzed cinnamaldehyde hydrogenation

M. Kołodziej, A. Drelinkiewicz, E. Lalik, J. Gurgul, D. Duraczyńska, R. Kosydar

Institute of Catalysis and Surface Chemistry, 30-239 Kraków, Niezapominajek 8, Poland

\* Corresponding author : A. Drelinkiewicz; [ncdrelin@cyf-kr.edu.pl](mailto:ncdrelin@cyf-kr.edu.pl)

**Graphical abstract****Highlights**

1. Hydrogenation of cinnamaldehyde catalysed by Pd/MoO<sub>3</sub> catalysts
2. Hydrogen bronzes and MoO<sub>3</sub> influenced either activity and selectivity of hydrogenation
3. Interaction of hydrogen with MoO<sub>3</sub> studied by microcalorimetric method
4. An optimum Pd-loading exists resulting in the best selectivity to aldehyde reduction

**Abstract**

Liquid phase hydrogenation of cinnamaldehyde (CAL) is studied at mild conditions (50<sup>0</sup>C, atmospheric pressure) on molybdena-supported Pd catalysts (0.5 – 4 wt % Pd) to elucidate an effect of hydrogen bronzes in controlling the selectivity to C=C/C=O hydrogenation. The Pd/SiO<sub>2</sub> catalyst is used as a reference, because SiO<sub>2</sub> is known to be an “inert” support. Additional information on the interaction of Pd/MoO<sub>3</sub> catalysts with hydrogen is provided by the microcalorimetric measurements. The impregnation of MoO<sub>3</sub> with palladium acetate followed by hydrogen reduction (250<sup>0</sup>C) produces Pd/MoO<sub>3</sub> catalysts containing Pd particles ca. 8-10 nm, regardless of the metal loading. The XRD, XPS, SEM, TEM, and HRTEM techniques have been employed to characterize the catalysts. The metal particles are nearly monodispersed and well distributed at low Pd-loading, 0.5 %Pd/MoO<sub>3</sub>. As the content of Pd increases the agglomeration of Pd particles occurs. All the Pd/MoO<sub>3</sub> catalysts display higher selectivity to C=O hydrogenation compared to Pd/SiO<sub>2</sub>. The content of Pd has an impact on activity and selectivity. The activity normalized to the Pd mass decreases with growing Pd-loading in Pd/MoO<sub>3</sub>. The C=C group of CAL was preferentially hydrogenated compared to the carbonyl (C=O) group at low (0.5 %Pd) and high (4%Pd) Pd content pointing out to an effect of optimum Pd-loading in the selectivity of CAL hydrogenation. The activity/selectivity behavior of Pd/MoO<sub>3</sub> catalysts is related to an effect of hydrogen bronzes existing during the catalytic tests. They could provide additional active sites efficient for the activation of CAL resulting in promotion of C=C hydrogenation. Hydrogen species in the bronzes could also have a beneficial effect on palladium crystallites formation upon reduction of palladium ions. High mobility of hydrogen species in the bronzes structure assisted by easy migration of palladium ions facilitated by MoO<sub>3</sub> layered morphology assisted by structural changes during the reduction could promote the Pd crystallites of tetrahedral shape.

Keywords: cinnamaldehyde hydrogenation, palladium, molybdena, hydrogen bronze

## 1. Introduction

A well known ability of  $\text{MoO}_3$  oxide to the formation of molybdenum bronzes ( $\text{H}_x\text{MoO}_3$ ) upon treatment by hydrogen has been widely investigated. The reduction of bulk  $\text{MoO}_3$  by molecular hydrogen occurs only at higher temperature (above  $300^\circ\text{C}$ ) [1, 2, 3] whereas in the presence of Pt or Pd particles, the bronzes formation begins already at ambient temperature and provides an opportunity to attain a high degree of hydrogen incorporation ( $1.55 < x < 1.72$ ) easily [1, 4]. The dissociation of  $\text{H}_2$  proceeds on the Pt/Pd particles, and then hydrogen is transported to the oxide phase by a spillover mechanism. The H atoms diffuse rather fast within the  $\text{H}_x\text{MoO}_3$  host lattice and they are bonded to the O atoms to form the O-H bonds. The small diffusion barriers for protons in the  $\text{MoO}_3$  lattice gives rise to high H-species mobility at near ambient temperature [5, 6, 7]. The detailed hydrogen spillover mechanism has also been studied by DFT calculation for Pt- $\text{MoO}_3$  [8] and Pd, Pt-clusters decorated  $\text{MoO}_3$  (010) [9]. The authors concluded that hydrogen diffusion may be slightly facilitated in case of larger metal clusters because of weaker metal-H interactions [9, 10]. The formation of hydrogen bronze phases was observed to proceed irrespective of reduction temperature and Pt-loading in the Pt/ $\text{MoO}_3$  samples [11]. However, apart from bronzes also certain lower oxides  $\text{MoO}_y$  ( $y < 3$ ), an oxyhydroxide  $\text{MoO}_{3-x}(\text{OH})_x$ , or a mixture of any of these may be formed [1]. It has been also observed that the formation of hydrogen molybdenum bronze makes the electronic structure of the compound metallic. Consequently, the structures formed upon high temperature treatment of  $\text{MoO}_3$  by hydrogen displayed catalytic activity via metallic as well as acid functions revealing in hydrogenation as well as isomerization and dehydration reactions. According to Al-Kandari et al [12, 13] the metallic function was result of  $\pi$  - bonding between adjacent Mo-Mo in the  $\text{MoO}_2$  whereas the hydrogen species of Mo-OH exhibited acid function. Partially reduced  $\text{MoO}_3$  was reported to be active for heptane isomerization [14,] dehydration and dehydrogenation of propan-2-ol [15]. Quite recent results show high activity of Rh- $\text{MoO}_3/\text{SiO}_2$  catalyst in hydrogenolysis of biomass-derived tetrahydrofurfuryl alcohol ascribed to catalytic action of acid sites from molybdenum bronze ( $\text{H}_{0.9}\text{MoO}_3$ ) assisted by that of metallic Rh [16].

Hydrogen bronze formed in the Pt/ $\text{MoO}_3$  sample has been demonstrated to serve as catalyst in hydrogenation of unsaturated C=C bonds in alkene reactant [17, 18, 19]. In fact, Marcq et al [19] found that hydrogenation of ethylene on  $\text{H}_{1.6}\text{MoO}_3$  formed in the Pt/ $\text{MoO}_3$  catalyst preceded without gaseous  $\text{H}_2$ . This experimental observation has been confirmed by the DFT calculations demonstrating that hydrogen molybdenum bronze of the  $\text{H}_x\text{MoO}_3(010)$  surface can be a highly effective catalyst for ethylene hydrogenation [10]. The weak physisorption of ethylene in the tilted configuration was found to be energetically most favorable due to the interaction between protonic H on the bronze surface and  $\pi$  electrons of ethylene. Zosimova et al [20] reported that hydrogen species migration via spillover mechanism in the Pt/ $\text{MoO}_3$  structure resulted in the formation of additional active sites involved in toluene hydrogenation. However, only those  $\text{MoO}_x$  particles that are in close vicinity to the Pt-particles took part in the formation of these additional active sites.

The activity/selectivity behavior of Pt/MoO<sub>3</sub> for acrolein hydrogenation has been observed to be strongly dependent on hydrogen activation temperature [21] which influenced the extent of the MoO<sub>3</sub> oxide reduction. The catalyst reduced below 160<sup>0</sup>C displayed similar catalytic performance to that of Pt/C. An enhanced selectivity to C=O obtained on high temperature (300-400<sup>0</sup>C) reduced Pt/MoO<sub>3</sub> was related to the new electron-deficient sites created as a result of an association of platinum atoms and electron-deficient molybdena cations. However, this high temperature reduction resulted in strongly decreased activity.

In the present paper we focus on the activity of Pd/MoO<sub>3</sub> catalysts in the hydrogenation of cinnamaldehyde (CAL), an example of  $\alpha,\beta$ -unsaturated aldehyde which could serve as a model compound to explore the role of hydrogen bronzes formed in the Pd/MoO<sub>3</sub> catalysts in a competition between C=C and C=O hydrogenation (Scheme 1). Hydrogenation of the former gives saturated aldehyde (hydrocinnamaldehyde, HCAL), the latter produces unsaturated alcohol (cinnamyl alcohol, COL) [22]. Apart from them, the fully saturated alcohol (HCOL) could be formed. The selectivity control is commonly related to the geometry of aldehyde adsorption on a metal theoretically studied by Delbecq et al. [23, 24]. A planar adsorption mode involving both C=C and C=O bonds favors hydrogenation of C=C yielding HCAL, while atop geometry involving the oxygen atom (C=O) promotes the formation of unsaturated alcohol (COL). The electron-deficient cation present in catalyst can act as an adsorption site for the C=O group of aldehyde thus improving the C=O selectivity. Promotion of C=O selectivity could be also attained using carriers like TiO<sub>2</sub>, CeO<sub>2</sub>, ascribed to the strong metal support interaction (SMSI) effect e.g. support-induced changes in reactivity of metal surface [25, 26]. An electron interaction between Pt, Pd particles and MoO<sub>3</sub> support is a well known phenomenon observed by number of authors [20, 27, 28]. Jackson et al [28] reported that platinum in the Pt/MoO<sub>3</sub> sample was positively charged (Pt <sup>$\sigma^+$</sup> ) due to metal –support interaction (SMSI). The Pt/MoO<sub>3</sub> catalysts displayed an enhanced sulfur tolerance [20], which is commonly related with the presence of electron deficient Pt <sup>$\sigma^+$</sup>  metal species [29].

The aim of this work is to study a role of MoO<sub>3</sub> – derived hydrogen bronzes in activity/selectivity pattern of CAL hydrogenation. The Pd/SiO<sub>2</sub> catalyst is used as a reference catalyst, because SiO<sub>2</sub> is known to be “inert” support and is not SMSI active. Additional information on the interaction of studied Pd/MoO<sub>3</sub> catalysts with hydrogen are provided by the microcalorimetric experiments.

## 2. Experimental

### 2.1. Catalysts preparation

Silica (Davisil 634, surface area 559 m<sup>2</sup>/g) and molybdenum oxide (Johnson Matthey, surface area 1.7 m<sup>2</sup>/g) were used as the supports. The catalysts were prepared by two methods: the colloid-based “water-in-oil” microemulsion and the impregnation methods. The 2%Pd/SiO<sub>2</sub> and 1%Pd/MoO<sub>3</sub>(ME)

catalysts were prepared by the reverse “water-in-oil” microemulsion method as described in details earlier [30]. Shortly, Pd particles were generated by addition of hydrazine (65 %) (molar ratio to Pd-ions of 20) to transparent dark orange microemulsion composed of PdCl<sub>2</sub> aqueous solution (0.2 mol/dm<sup>3</sup>), cyclohexane and surfactant (Triton-X 114) at water/surfactant molar ratio  $w = 5$ . Deposition of Pd particles on support was carried out by very slow THF adding to vigorously stirred suspension of support in the Pd-containing microemulsion. Finally, the catalysts were washed with acetone, methanol and water up to the removal of chloride ions, dried at 120<sup>0</sup>C for 16 h.

All other catalysts with Pd loading from 0.5 wt % up to 4 wt% were prepared by impregnation of MoO<sub>3</sub> support with acetone solution of Pd(ac)<sub>2</sub>. The appropriate amount of Pd-solution was added into support and the obtained suspension was slowly evaporated upon heating up to evaporation of liquid. Then, the obtained yellow sample was dried in air for 24 h and reduced with hydrogen (5 % H<sub>2</sub> in N<sub>2</sub>) at temperature of 250<sup>0</sup>C (3 h) and stored in contact with air.

## ***2.2. Methods of characterization***

**The X-ray diffraction (XRD)** patterns were obtained with a Philips X'PERT diffractometer using Cu K $\alpha$  radiation (40 kV, 30 mA). The average diameter of Pd particles was calculated on the basis of the Pd (111) peak broadening according to Scherrer equation (taking into account instrumental broadening).

**The X-ray Photoelectron Spectroscopy (XPS)** measurements were carried out with a hemispherical analyzer (SES R4000, GammaData Scienta). The unmonochromatized Al K $\alpha$  and Mg K $\alpha$  X-ray source with the anode operating at 12 kV and 20 mA current emission was applied to generate core excitation. All binding energy values were corrected to the carbon C 1s excitation at 285.0 eV. The samples were pressed into indium foil and mounted on a holder. All spectra were collected at pass energy of 100 eV except survey scans which were collected at pass energy of 200 eV. Intensities were estimated by calculating the integral of each peak, after subtraction of the Shirley- type background, and fitting the experimental curve with a combination of Gaussian and Lorentzian lines of variable proportions (70:30).

**Electron Microscopy (SEM, TEM)** studies were performed by means of Field Emission Scanning Electron Microscope JEOL JSM – 7500 F equipped with the X-ray energy dispersive (EDS) system. Two detectors were used and the images were recorded in two modes. The secondary electron detector provided SEI images, and back scattered electron detector provided BSE (COMPO) micrographs.

HRTEM and STEM studies were performed on FEI Tecnai G<sup>2</sup> transmission electron microscope operating at 200 kV equipped with EDAX EDX and HAADF/STEM detectors. Samples for analysis were prepared by placing a drop of the suspension of sample in ethanol or THF onto a carbon-coated copper grid, followed by evaporating the solvent.

**Microcalorimetric experiments** were performed using Microscal gas flow-through microcalorimeter. The instrument has been designed to measure thermal effects of solid/gas interactions concurrently

with the gas uptake at constant temperature. The design as well as operation of the instrument has been previously described in detail [31] and the use of Microscal microcalorimeter in studying the thermal effects in catalytic reaction of hydrogen and oxygen on noble metals and in hydrogen sorption by oxides have also been reported [32, 33]. The instrument design makes it possible to use in-situ calibration pulses of controlled power and duration, thus yielding a calibration factor for each individual experiment. The amount of evolving heat was monitored vs reaction time, and concurrently the uptake of hydrogen was measured using thermoconductivity detector (TCD) located down-stream of the cell. The average molar heat (kJ/mol H<sub>2</sub>) was calculated as a ratio of the total evolved heat and the total number of hydrogen moles consumed. The amount of the catalyst used to fill the microcalorimetric cell (ca. 0.15 cm<sup>3</sup>) was ca. 0.2 g. The process of sorption of hydrogen was carried out at temperature of 22<sup>0</sup>C and under atmospheric pressure using 5% H<sub>2</sub> in N<sub>2</sub>, flow rate 3 cm<sup>3</sup>/min. The process of hydrogen uptake was studied for 2%Pd/MoO<sub>3</sub> catalyst and the physically mixed 2%Pd/MoO<sub>3</sub> + MoO<sub>3</sub> (1/1 by weight).

### 2.3. Hydrogenation reactions

Hydrogenation experiments were carried out in an agitated batch glass reactor at constant atmospheric pressure of hydrogen following the methodology previously described [34]. Toluene was used as the solvent. The catalyst was activated "in situ" prior to its contact with CAL-containing solution. After having been placed in reactor the dry sample of catalyst was wetted with toluene, and then activated by purging first with nitrogen (20 min; ambient temperature) and subsequently with hydrogen at temperature of 22<sup>0</sup>C (15 min) and 50<sup>0</sup>C (20 min). In experiments using the Pd/MoO<sub>3</sub> + MoO<sub>3</sub> mixture as catalyst, both components were mixed thoroughly before being placed in the reactor. For the experiments carried out at lower temperatures (23 – 44<sup>0</sup>C), the catalyst was activated only at 50<sup>0</sup>C. The reaction was started after cooling the system under hydrogen flow to desired temperature.

The progress of the reaction was monitored by measuring the hydrogen consumed against reaction time. Samples of solutions were withdrawn from the reactor and analysed using GC chromatograph PE Clarus 500, with a flame ionisation detector and capillary column Elite-5 MS (30 m x 0.25 mm x 0.25 μm coating). The conditions of analysis: helium as a carrier gas (flow rate 1.5 ml/min), injection temperature 300 °C, temperature ramp 65<sup>0</sup>C for 1 min, 65–108<sup>0</sup>C (15<sup>0</sup>C/min), 108–115 (5<sup>0</sup>C/min), 105<sup>0</sup>C hold for 7 min, 115–265 (30<sup>0</sup>C/min), 265<sup>0</sup>C hold for 3 min. Decane (Sigma Aldrich) was used as the standard.

Typically the hydrogenation test was carried out at 50<sup>0</sup> C using 20 cm<sup>3</sup> in cinnamaldehyde solution in toluene of  $c^0 = 0.05 \text{ mol/dm}^3$  and catalyst concentration 5 g/dm<sup>3</sup>. The same conditions were used in the hydrogenation of HCAL as the substrate.

The conversion (C; %), selectivity to hydrocinnamaldehyde [S(HCAL); %], saturated alcohol [S(HCOL); %] were calculated with the formulas

$$C_{\text{CAL}} = (N_{\text{CAL},0} - N_{\text{CAL}} / N_{\text{CAL},0}) \times 100 \% \quad (1)$$

$$S_i = (N_i / N_{\text{CAL},0} - N_{\text{CAL}}) \times 100 \% \quad (2)$$

where  $N_{\text{CAL},0}$  and  $N_{\text{CAL}}$  are the moles of CAL initially present in the reactor and the moles of CAL remaining at time  $t$ , respectively;  $N_{\text{HCAL}}$ ,  $N_{\text{HCOL}}$  are the numbers of moles of hydrocinnamaldehyde (HCAL) and saturated alcohol (HCOL) in the reaction mixture at time  $t$ .

Shaking of the reactor was carried out at such a speed to ensure that the rate of hydrogen uptake did not depend on agitation speed. External diffusion resistance was ruled out, since no significant variation in the catalytic results was observed by increasing the agitation speed.

### 3. Results and discussion

#### 3.1. Preparation and characterization of catalysts

The very low specific surface area of  $\text{MoO}_3$  (lower than  $2 \text{ m}^2/\text{g}$ ) is a great disadvantage for preparation of catalysts with well dispersed metal (Pt, Pd) particles. The analysis of literature shows that to reach a metal content of 0.5-1 wt%, several consecutive impregnations should be performed. Hoang-Van et al. [21] obtained finely dispersed Pt particles (few nm in size) in the Pt/ $\text{MoO}_3$  catalyst but metal loading was as low as 0.1 mol %. Zosimova et al. [20] synthesized the Pt- $\text{MoO}_3$  catalysts by oxidation of Pt – Mo alloy precursors. This method was more effective, as it produced catalysts of higher Pt loading with Pt particles of 19-35 nm in size. Therefore, Pt and  $\text{MoO}_3$  dispersed over carriers such as alumina, silica, zeolites, or other were usually applied.

In the present work two preparation methods are used. The colloid-based “water-in-oil” reverse microemulsion (ME) method was used for preparation 2%Pd/ $\text{SiO}_2$  and 1%Pd/ $\text{MoO}_3$ (ME) catalysts. All other Pd/ $\text{MoO}_3$  catalysts (0.5 - 4 wt % Pd) were prepared by impregnation using  $\text{Pd}(\text{ac})_2$  as the precursor followed by reduction with  $\text{H}_2$  at  $250^\circ\text{C}$  (3 h). The ME method allows preparation of metal particles of precisely predicted size in a narrow range [35, 35]. According to this method, at first metal particles are generated in the microemulsion medium and then they are deposited onto the support. Consequently, the size of metal particles in the supported catalysts is almost the same, regardless of the type of support and metal loading [37]. Therefore, Pd particles of the same average size could be expected in both 2%Pd/ $\text{SiO}_2$  and 1%Pd/ $\text{MoO}_3$ (ME) catalysts.

In the XRD pattern of 2%Pd/ $\text{SiO}_2$  catalyst the diffractions of crystalline Pd at  $2\theta$   $40.16^\circ$  and  $2\theta$   $46.7^\circ$  are visible (Fig. S 1). The average Pd particle size calculated from the peak broadening using the Scherrer equation is determined to be ca. 8.5 nm. The electron microscopy image of 2%Pd/ $\text{SiO}_2$  catalyst (Fig. S 2) show nearly monodispersed and rather evenly distributed individual Pd particles accompanied by only few larger “white spots” of slightly aggregated nanoparticles. On the other hand, in the Pd/ $\text{MoO}_3$ (ME) catalyst the individual metal particles only occasionally appear while the aggregates of various shapes dominate (Fig. S 2). They are composed of individual spherical metal

particles of almost uniform size, which can be roughly estimated to be ca. 8 - 10 nm. A strong aggregation of particles may be result of very low specific surface area of MoO<sub>3</sub>, 1.7 m<sup>2</sup>/g, distinctly lower than that of silica support, 559 m<sup>2</sup>/g.

In the XRD patterns of hydrogen reduced Pd/MoO<sub>3</sub> catalysts prepared by impregnation method (Fig. 1) a set of strong reflections from the MoO<sub>3</sub> appears. The strong MoO<sub>3</sub> reflections and in particular the ones located in the 2θ region of 39 - 40° make difficult an observation of the Pd crystalline lines. Furthermore, it has been reported, that reflections from crystalline Pt of 6.5 nm in size were observable in the MoO<sub>3</sub> support only at high metal loading, above 10 wt% in this case [38]. The XRD pattern of 1%Pd/MoO<sub>3</sub> catalyst (Fig. 1) does not show apparent presence of Pd crystallites. Some changes within the 2θ region of Pd-line can be seen at higher Pd loading, 2 and 4 wt % Pd, more distinctly observable in the inset showing the section between 38 and 41°. A broadening accompanied by a rising of the base line is visible for 2%Pd/MoO<sub>3</sub> and Pd diffraction is much better shaped in the 4%Pd/MoO<sub>3</sub> catalyst.

The XRD patterns also show a gradual broadening of the MoO<sub>3</sub> diffractions with growing Pd-loading thus evidencing some morphological changes of initial MoO<sub>3</sub> oxide during reduction (Fig. 1). They resulted also in increase of specific surface area to 7 m<sup>2</sup>/g for 2%Pd/MoO<sub>3</sub> catalyst relative to 1.7 m<sup>2</sup>/g of initial sample. These changes are consisted with previous data reporting an increase of surface area and amorphization of Pt or Pd-MoO<sub>3</sub> samples upon hydrogen treatment [39, 40, 41].

No diffractions lines originating from lower oxides like MoO<sub>2</sub> phase (2θ = 26.°, 36.9, 53.7°) can be seen in the diffraction pattern of Pd/MoO<sub>3</sub> catalysts (Fig. 1), consistent with previous studies devoted to the temperature effect upon hydrogen treatment of Pd/MoO<sub>3</sub> [41] and Pt/MoO<sub>3</sub> [1, 42]. The reduction to lower oxides was not observed upon hydrogen treatment of Pt/MoO<sub>3</sub> below 200°C [1, 42]. The Pd/MoO<sub>3</sub> catalyst reduced at 350°C gave no diffraction lines of MoO<sub>2</sub> phase whereas small diffractions related to hydrogen molybdenum bronze appeared [41].

In the patterns of Pd/MoO<sub>3</sub> catalysts (Fig. 1) low intense reflections from the hydrogen bronzes also appear [2, 43, 44]. They could be identifying as traces of H<sub>0.34</sub>MoO<sub>3</sub> (00-034-1230) in all the catalysts, irrespective of the Pd-loading, from 1%Pd up to 4%Pd.

The Pd/MoO<sub>3</sub> catalysts after reduction with H<sub>2</sub> were stored in contact with air. It is well known, that hydrogen bronzes re-oxidize in contact with air at ambient temperature [1]. The bronze with the highest hydrogen content changed successively to that with lower hydrogen content and finally to MoO<sub>3</sub>, whereas re-oxidation under mild conditions does not lead to oxygen deficient oxides [45]. The H<sub>1.6</sub>MoO<sub>3</sub> sample displayed high instability and easily re-oxidized to H<sub>0.9</sub>MoO<sub>3</sub> at ambient temperature [38] whereas the oxidation process was very slow for bronzes of H-content below 0.9 [38, 45]. This could explain why there are only very low intense diffractions arising from the hydrogen bronzes in the pattern of studied Pd/MoO<sub>3</sub> catalysts (Fig. 1)

Fig. 2 shows the SEM micrographs of Pd/MoO<sub>3</sub> catalysts synthesized using Pd(ac)<sub>2</sub> precursor and reduced with hydrogen (at 250°C). The morphology of bulk MoO<sub>3</sub> composed of layers of slabs

parallel to the basal (010) plane forming layered, plate-type structure is clearly observable in the micrograph of initial MoO<sub>3</sub> support. This plate-type morphology is still preserved in the Pd-containing catalysts. Non-aggregated, individual Pd particles nearly evenly distributed on the MoO<sub>3</sub> surface predominate in studied catalysts. The location of Pd particles seems to be related with morphological features of the MoO<sub>3</sub>. Majority of particles is located on the surface of molybdena plates. Remarkably, a fraction of the particles form parallel arrangements, apparently located along the edges of the plates. Most of the Pd particles are of spherical shape commonly observed in the case of polyhedral (octahedral) nanocrystalline Pd. However, apart from them, a few crystalline particles of well developed tetrahedral shape can be observed. It should be stressed that palladium nanocrystals of tetrahedral shape are very rarely observed. Their formation is less favorable because of much larger (by 1.3 times) surface to volume ratio relative to that in commonly formed particles of octahedron shape [46]. There are a few reports on the synthesis of metal particles with tetrahedral shape but the mechanism of growth has not yet been revealed. Recent study by Wang et al [46] demonstrates that Pd nanocrystals of different shapes, octahedrons or tetrahedrons could be obtained by manipulating the reduction kinetics of a palladium precursor. A slow reduction of Na<sub>2</sub>PdCl<sub>4</sub> precursor ensure thermodynamically controlled growth of octahedrons while fast reduction of Pd(acac)<sub>2</sub> directed the crystal growth into a kinetically controlled mode yielding well shaped tetrahedral Pd nanocrystals [46]. Similar conclusion that kinetic control in reduction process is required to form tetrahedral Pd nanostructures was reported in recent papers of Zhu et al [47].

It might be supposed that high mobility of hydrogen species in the bronzes structure accompanied by facilitated palladium ions migration due to layered MoO<sub>3</sub> morphology assisted by structural changes during the reduction process could favor the tetrahedral Pd nanostructures. This phenomenon although seems to be very interesting from the catalytic point of view, it needs more detailed investigations.

The TEM micrographs show palladium particles of size in a narrow range, evaluated to be ca. 8 – 10 nm regardless the Pd-loading, in the 0.5%Pd/MoO<sub>3</sub> as well as in the 4%Pd/MoO<sub>3</sub> catalysts (Fig. 3). It indicates that Pd-loading does not essentially affect the size of Pd particles. However, with growing Pd-loading more and more palladium particles form small aggregates consisting of few particles which could be clearly observable in the 4%Pd/MoO<sub>3</sub> catalyst.

The 0.5%Pd/MoO<sub>3</sub> and 4%Pd/MoO<sub>3</sub> catalysts (reduced with hydrogen) are also subjected to the X-ray photoelectron spectroscopy (XPS) experiments. The binding energy of Pd 3d<sub>5/2</sub> in both catalysts is observed within similar range of 335 - 336 eV (Fig. S 3). The peak component at ca. 335 eV characteristic of metallic Pd dominates in the spectra of both catalysts. Apart from the Pd-metal state, there appears also a less intense peak component at slightly higher energy of ca. 336 - 337 eV. This peak component likely results from palladium – molybdenum oxide interactions, consistent with previous observations [20, 27, 28]. However, partially oxidized Pd<sup>δ+</sup> species on the metal particles surface are commonly characterized by the binding energies slightly above 336 eV.

In the XPS Mo 3d<sub>5/2</sub> spectrum of initial MoO<sub>3</sub> (Fig. S 3) the peak at binding energy of 233.11 eV commonly ascribed to Mo(VI) strongly dominates. The binding energy of Mo(VI) could be observed within the range 232.6 – 233.7 eV depending on oxygen surrounding and coordination [48, 49]. A small contribution of Mo 3d<sub>5/2</sub> peak component of lower energy 231.34 eV indicates some amount of Mo-species of lower oxidation number [50]. The Mo 3d<sub>5/2</sub> energy of 231.4 eV could be related to Mo(IV) species in view of the linear relation between the binding energies and the oxidation number of Mo states with a slope of 0.8 eV per oxidation state found by Grunert et al [50].

The more complex structure of the Mo(3d) energy region can be seen in the XPS spectra of 0.5%Pd/MoO<sub>3</sub> and 4%Pd/MoO<sub>3</sub> catalysts. In the 0.5%Pd/MoO<sub>3</sub> catalyst the share of Mo(VI) decreases at the expense of growing contributions of partially reduced molybdenum species which according to the above-mentioned relation [50] could be ascribed to Mo(V). A contribution of these partially reduced Mo-species in the 4%Pd/MoO<sub>3</sub> catalyst is definitively lower. Upon hydrogen treatment resulting in the hydrogen intercalation process, molybdenum is being reduced, and this was reflected in the Mo 3d<sub>5/2</sub> components of binding energy lower compared to Mo(VI) [28]. It should be noted that hydrogen treated 0.5%Pd/SiO<sub>2</sub> and 4%Pd/MoO<sub>3</sub> catalysts were stored in air, e.g. at conditions facilitating hydrogen bronzes re-oxidation and the diffraction lines of hydrogen bronzes are of very low intensity in their XRD pattern (Fig. 1). Nevertheless, relatively low contribution of partially reduced molybdenum species detected in the surface of catalyst with high Pd-loading (4%Pd) may suggest more effective decomposition of hydrogen bronzes due to higher Pd-content. However, some contribution of partially reduced Mo-species in surface of catalysts which could be formed during hydrogen reduction at temperature of 250<sup>0</sup>C can not be excluded.

### 3.2. Catalytic results

#### Hydrogenation of cinnamaldehyde (CAL)

Palladium is known to exhibit high reactivity for the double C=C bond hydrogenation. Consequently, in the presence of Pd catalysts, saturated aldehyde, hydrocinnamaldehyde (HCAL) is commonly observed as the dominating product [22].

In the presence of all studied catalysts, the saturated aldehyde (HCAL) and saturated alcohol (HCOL) are observed from the very beginning of the reaction. No cinnamyl alcohol (COL) is detected at the present reaction conditions (toluene, 50<sup>0</sup>C, atmospheric hydrogen pressure) consistent with previous observations for Pd catalysts [51-54]. In hydrogenation of CAL on Pd/SiO<sub>2</sub> catalyst at mild conditions (25<sup>0</sup>C, atmospheric pressure), all saturated alcohol (HCOL) was formed entirely through the consecutive hydrogenation of the cinnamyl alcohol [51, 53], because the hydrogenation of COL reactant to saturated alcohol was ca. 30-times faster than the hydrogenation of CAL to cinnamyl alcohol. It has been related to much higher palladium reactivity to unsaturated C=C bond hydrogenation than that to C=O [22, 25].

Based on these literature data, the control hydrogenation experiments on 2%Pd/SiO<sub>2</sub> and 2%Pd/MoO<sub>3</sub> catalysts have been performed using HCAL as the substrate. On both catalysts, the hydrogenation of HCAL at 50<sup>0</sup>C has not produced any detectable amount of saturated alcohol (HCOL). The concentration of HCAL in the reaction mixture has not decrease and no consumption of hydrogen has appeared during catalytic tests lasting up to 4-6 h. Thus, the obtained results are consistent with previous data and indicate that under present reaction conditions saturated alcohol HCOL is produced exclusively from the hydrogenation of COL.

The MoO<sub>3</sub> sample did not exhibit activity for CAL hydrogenation, similarly to what was observed in acrolein hydrogenation using low temperature (50<sup>0</sup>C) activated MoO<sub>3</sub> [21]. The obtained catalytic results indicate that MoO<sub>3</sub> support plays an important role in determining the course of CAL hydrogenation in terms of both, the rate and the selectivity towards C=C/C=O hydrogenation. The method of catalysts preparation as well as the Pd loading in the MoO<sub>3</sub>-supported catalysts, both are the variables determining the catalytic behavior, and in particular the selectivity of CAL hydrogenation. Among all studied catalysts, the 2%Pd/SiO<sub>2</sub> displays the highest selectivity to C=C hydrogenation which is as high as ca. 85 % (Fig. S 4) and is almost constant throughout the reaction. This behavior is consistent with much higher Pd reactivity toward C=C bond hydrogenation compared to that to C=O.

1%Pd/MoO<sub>3</sub>(ME) catalyst prepared by the “reverse“ microemulsion method with strongly aggregated Pd particles exhibits very low activity assisted by preferential hydrogenation of C=C (Fig. 4) giving selectivity to HCAL ca. 75 %, which is slightly lower than that on the 2%Pd/SiO<sub>2</sub> catalyst (85%). This high selectivity to C=C hydrogenation on 1%Pd/MoO<sub>3</sub>(ME) is almost preserved during the whole CAL conversion similarly to 2%Pd/SiO<sub>2</sub>. This similar behavior could be related to poor Pd dispersion in the 1%Pd/MoO<sub>3</sub>(ME) catalyst. A lack of a good contact between the palladium and the MoO<sub>3</sub> surface results in strongly limited electron interaction and modification of metal active sites towards CAL adsorption.

The palladium is much better dispersed in all the catalysts prepared by the impregnation method (Fig. 2, 3). Consequently, the 1%Pd/MoO<sub>3</sub> catalyst prepared by the latter method is much more active than the 1%Pd/MoO<sub>3</sub>(ME) sample (Fig. 4). As the Pd loading in the Pd/MoO<sub>3</sub> catalysts grows from 0.5 wt% up to 4 wt% Pd, the rate of CAL conversion grows. As a measure of catalyst activity, we use the initial rate of CAL hydrogenation normalized to the Pd mass (mol CAL/ min<sup>-1</sup> g<sup>-1</sup> Pd) and we call such parameter "specific activity" (SPC). Its change with Pd-loading in the Pd/MoO<sub>3</sub> catalysts is displayed in Fig. 4 c. For comparison, the activity (SPC) data obtained on 2%Pd/SiO<sub>2</sub> and 1%Pd/MoO<sub>3</sub>(ME) catalysts are also reported. The specific activity is the highest at the lowest Pd-content (0.5%Pd) and it gradually decreases with growing Pd loading up to 2%Pd/MoO<sub>3</sub> catalyst. However, the SPC clearly stabilizes on further growth in the Pd loading, and hence the values of SPC for 2%Pd/MoO<sub>3</sub> and 4%Pd/MoO<sub>3</sub> catalysts are almost the same (1.18 x 10<sup>-2</sup> and 1.15 x 10<sup>-2</sup> mol CAL min<sup>-1</sup> g<sup>-1</sup> Pd, respectively). They are also comparable to that obtained for 2%Pd/SiO<sub>2</sub> catalyst (1.20 x 10<sup>-2</sup> mol CAL min<sup>-1</sup> g<sup>-1</sup> Pd) (Fig. 4 c).

The size of Pd particles does not essentially differ in all the Pd/MoO<sub>3</sub> catalysts. However, the extent of Pd particles aggregation gradually increases with growing Pd loading and aggregated particles can be seen in the 4 %Pd/MoO<sub>3</sub> catalyst (Fig. 2). However, the activity change reported in Fig. 4 c is too strong to be related to the effect of Pd-aggregation only.

The MoO<sub>3</sub> support has an impact on the way CAL is reacted. In comparison with Pd/SiO<sub>2</sub>, all Pd/MoO<sub>3</sub> catalysts offer higher selectivity to saturated alcohol (HCOL) and lower towards C=C hydrogenation. However, the selectivity is dependent on Pd-loading in the Pd/MoO<sub>3</sub> catalysts (Fig. 4 b). At the lowest Pd loading, e.g. 0.5%Pd/MoO<sub>3</sub> catalyst the selectivity to C=C hydrogenation is high 75 – 65 %, and it slowly decrease as the CAL conversion grows. At higher Pd loading 0.75% and 1%Pd, the selectivity toward C=C hydrogenation decreases and on 1%Pd/MoO<sub>3</sub> attains the lowest level, ca. 45-50% among all MoO<sub>3</sub>-supported catalysts. On 1%Pd/MoO<sub>3</sub> catalyst, the content of saturated alcohol (HCOL) is almost equal or even exceeds that of saturated aldehyde (HCAL) at complete CAL conversion. On further increase of Pd-loading to 2 and 4 wt % Pd, the selectivity toward C=C hydrogenation yielding saturated aldehyde (HCAL) grows again. As the result, on 4%Pd/MoO<sub>3</sub> catalyst the selectivity to C=C hydrogenation is high 60-65 %, however it is lower than that on the 2%Pd/SiO<sub>2</sub> catalyst. Thus, selectivity pattern of CAL hydrogenation is strongly determined by the Pd-loading in the Pd/MoO<sub>3</sub> catalysts. A promotion of C=O hydrogenation in the CAL reactant could be obtained but an optimum Pd loading is needed. In the present catalysts the best C=O promotion effect is obtained on 1%wt Pd-containing catalyst.

The XRD patterns registered for 2%Pd/MoO<sub>3</sub> and 4%Pd/MoO<sub>3</sub> catalysts after the catalytic experiments are reported in Fig. 5. The sample of catalyst taken from the reactor was washed with acetone and dried in air at room temperature. After this operation lasting ca. 0.5 h a part of the sample was subjected to the XRD studies. The next XRD patterns were registered for the samples allowed to be in contact with air for 48 h and 20 days.

The first XRD pattern registered after ca. 0.5 h is quite different form that of initial 2%Pd/MoO<sub>3</sub> catalyst (Fig. 5). The distinct diffraction lines characteristic of the H<sub>0.9</sub>MoO<sub>3</sub> appear whereas there are no reflections from the MoO<sub>3</sub>. Upon contacting the catalyst with air its XRD pattern gradually changes due to the re-oxidation and the diffraction lines characteristic of the H<sub>0.34</sub>MoO<sub>3</sub> and those of MoO<sub>3</sub> are observed after 48 h. An almost complete transformation to the MoO<sub>3</sub> phase is evidenced by the set of diffraction lines of MoO<sub>3</sub> in the XRD pattern registered after 20 days. Similarly, the diffraction lines of H<sub>0.34</sub>MoO<sub>3</sub> and lack of those arising from MoO<sub>3</sub> can be seen in the XRD pattern registered after 24 h for the recovered 4%Pd/MoO<sub>3</sub> catalyst.

This is consistent with the results reported by Matsuda et al [55] for different content of Pd and Pt-containing MoO<sub>3</sub> samples (0.001 – 0.1 mol % Pd, Pt). During treatment of Pt/MoO<sub>3</sub> (0.001 mol %Pt) in H<sub>2</sub> flow at room temperature the H<sub>0.34</sub>MoO<sub>3</sub> and H<sub>0.93</sub>MoO<sub>3</sub> phases were formed and the high Pt-containing Pt/MoO<sub>3</sub> catalyst (0.1 mol% Pt) was converted to H<sub>1.68</sub>MoO<sub>3</sub> phase. Hence, it could be concluded from the obtained XRD results that upon activation of catalyst with hydrogen “in situ” (at

50°C) prior to the catalytic test, hydrogen molybdenum bronzes were formed. On the other hand, the reduction of Mo(VI) in the catalysts to lower valence states should be essentially avoided because of low temperature of “in situ” activation (50°C). Marcq et al [19] reported that treatment of Pt/MoO<sub>3</sub> catalysts at low temperature e.g. 60°C does not result in the formation of water, confirmed for bronze with H/Mo = 1.5.

To gain insights into the role of hydrogen bronzes in activity/selectivity behavior of MoO<sub>3</sub>-supported catalysts the set of experiments including the effect of catalyst concentration, initial CAL concentration and apparent activation energy are performed. Furthermore, the stability of catalyst is also checked. As shown in Fig. 6, reusing of the 2%Pd/MoO<sub>3</sub> catalyst resulted in almost the same activity/selectivity pattern as the one obtained in the first catalytic test. Such stable performance indicates that Pd-phase does not essentially change under present reaction conditions.

The initial rate of CAL hydrogenation normalized to 1 g of catalyst obtained at various concentrations of 2%Pd/MoO<sub>3</sub> catalyst is almost constant (Fig. S 5) as well as the selectivity pattern of CAL conversion is preserved. This indicates that no external mass transfer effect operates under applied conditions. An influence of internal diffusion seems to be unlikely due to very low specific surface area of MoO<sub>3</sub> (1.7 m<sup>2</sup>/g).

Within the whole range of initial CAL concentrations (0.02 – 0.08 mol/dm<sup>3</sup>) the initial rate of CAL hydrogenation on 2%Pd/MoO<sub>3</sub> is almost the same and the selectivity pattern is preserved (Fig. S 5). It shows zero-order of reaction with respect to CAL concentration, in agreement with results on Pd/SiO<sub>2</sub> [52] and Pd/C catalysts [56, 57] obtained in toluene solvent.

With rising reaction temperature (23 – 60 °C) the rate of CAL hydrogenation on 2%Pd/MoO<sub>3</sub> increases whereas the temperature of reaction does not influence the selectivity pattern of CAL conversion. Using initial rates of CAL conversion (below ca. 10 % conversion) the apparent activation energy was estimated. The Arrhenius plot (Fig. 7) turned out to be linear throughout the whole temperature range (23 – 60°C), and the apparent activation energy has been calculated to be 52 kJ/mol. At similar reaction conditions (toluene solvent, 20 - 70°C), somewhat higher values of activation energies, namely 60+/-5 kJ/mol on 5%Pd/C commercial [57], 60 kJ/mol on Pd-mesoporous silica [58] and 70 kJ/mol on Pd/various carbon materials [54] are reported.

### **Physical mixture of Pd/MoO<sub>3</sub> and MoO<sub>3</sub>**

As described before, the MoO<sub>3</sub> sample itself was inactive for the CAL hydrogenation under the conditions used. However, significant synergistic effect appears for physically mixed systems of Pd/MoO<sub>3</sub> catalyst and MoO<sub>3</sub> sample (at 1:1 mass ratio). The effect of added MoO<sub>3</sub> is studied for 1%Pd/MoO<sub>3</sub> and 2%Pd/MoO<sub>3</sub> catalysts

As shown in Fig. 6 for both physically mixed Pd/MoO<sub>3</sub> + MoO<sub>3</sub> systems consisting of 1%Pd/MoO<sub>3</sub> or 2%Pd/MoO<sub>3</sub> catalysts the rates of CAL hydrogenation is accelerated relative to that on

pure Pd/MoO<sub>3</sub> catalysts. At the same amount of MoO<sub>3</sub> mixed with the 1%Pd/MoO<sub>3</sub> and 2%Pd/MoO<sub>3</sub> catalysts the rate increases 1.6 and 1.3 – times, respectively.

It is interesting that on physically mixed Pd/MoO<sub>3</sub> + MoO<sub>3</sub> systems the significant selectivity growth in C=C selectivity is attained, observed within the whole CAL conversion range (Fig. 6). In both reaction systems, with 1%Pd/MoO<sub>3</sub> and 2%Pd/MoO<sub>3</sub> catalysts, almost the same growth of selectivity due to the same amount of added MoO<sub>3</sub> is obtained, equal to 12 %.

The XRD pattern of recovered 2%Pd/MoO<sub>3</sub> + MoO<sub>3</sub> sample (after the catalytic test) (Fig. 5) shows apart from the diffraction lines characteristic of MoO<sub>3</sub>, also the reflections from various hydrogen bronzes, such as H<sub>0.34</sub>MoO<sub>3</sub> and H<sub>0.9</sub>MoO<sub>3</sub>. This result could be an experimental evidence of hydrogen bronzes formation in hydrogenation test carried out with Pd/MoO<sub>3</sub> + MoO<sub>3</sub> mixture. In typical procedure of catalytic tests, the catalyst was activated “in situ” by passing hydrogen at temperature of 22<sup>0</sup>C (15 min) and 50<sup>0</sup>C (20 min) before the reaction. The control hydrogenation experiment in which the sample of 2%Pd/MoO<sub>3</sub> + MoO<sub>3</sub> was activated by hydrogen at 50<sup>0</sup>C for longer time, 60 min was also performed. The obtained activity and selectivity data do not essentially differ from those obtained in catalytic tests carried out by typical procedure (Fig. 6). This seems to suggest, that the hydrogen bronze formation is completed at typical conditions of hydrogen activation stage.

For the 2%Pd/MoO<sub>3</sub> + MoO<sub>3</sub> mixture (weight ratio of 1:1) the effect of reaction temperature (23 – 50<sup>0</sup>C) is also studied. In all experiments the activation by hydrogen was carried out with the same procedure (under H<sub>2</sub> flow 15 min at 22<sup>0</sup>C and 20 min at 50<sup>0</sup>C). Within the whole range of reaction temperatures, the rate of CAL hydrogenation on the Pd/MoO<sub>3</sub> + MoO<sub>3</sub> is ca. 1.6 – times higher than on 2%Pd/MoO<sub>3</sub> alone. In the presence of added MoO<sub>3</sub> the selectivity pattern of CAL hydrogenation is preserved within the whole temperature range. From the Arrhenius plot (Fig. 7) the apparent activation energy of CAL hydrogenation Pd/MoO<sub>3</sub> + MoO<sub>3</sub> is calculated to be 52.5 kJ/mol, which is almost the same as that of CAL hydrogenation (52 kJ/mol) on Pd/MoO<sub>3</sub> alone.

The Arrhenius plots on 2%Pd/MoO<sub>3</sub> catalyst studied alone or with added MoO<sub>3</sub>, both are linear and parallel within the whole temperature range. These relations show that the pre-exponential factor in the CAL hydrogenation on physically mixed Pd/MoO<sub>3</sub> + MoO<sub>3</sub> is higher than that calculated for the Pd/MoO<sub>3</sub> alone. The same effect in the activation energy and pre-exponential factor was observed in other reactions, namely hydrogenation of benzene and 1,3-butadiene on various Pd-Au catalysts [59] and oxidation of CO on Co-based catalysts [60]. It has been explained assuming that the active sites are identical evidenced by the same activation energy whereas higher content of the sites generates the growth of pre-exponential factor [60]. In view of these observations, it could be supposed that active sites for CAL hydrogenation in both reaction systems with and without added MoO<sub>3</sub> are the same whereas their concentration grows in the experiment with added MoO<sub>3</sub>.

A positive impact of TiO<sub>2</sub> addition was also observed by Liu et al [61] in citral hydrogenation on the Pd/TiO<sub>2</sub> catalyst. The addition of neat TiO<sub>2</sub> was effective for increasing the total citral conversion

along with an increase in the selectivity to C=C hydrogenation. This synergistic effect has been related with the presence of spill-over hydrogen facilitated by the TiO<sub>2</sub> support.

### Microcalorimetric experiments

The gas flow-through microcalorimetry makes it possible to measure the rate of heat evolution accompanying the sorption of hydrogen concurrently with the rate of hydrogen uptake in the catalyst sample. The results obtained in our previous work showed that hydrogen sorption by the PdPt/MoO<sub>3</sub> catalyst [33] was an exothermic process, consistent with literature data [1, 62, 63]. The amount of sorbed hydrogen was determined to be 0.85 mol H<sub>2</sub> per mol MoO<sub>3</sub>, corresponding to the H<sub>1.7</sub>MoO<sub>3</sub> stoichiometry of the bronze [33]. The amount of evolved heat accompanying its formation was determined to be 97 kJ/mol H<sub>2</sub>, similar to 105 kJ/mol H<sub>2</sub> reported for the H<sub>1.6</sub>MoO<sub>3</sub> bronze. The systematic studies reported by Noh et al. [62] demonstrated that incorporation of hydrogen into MoO<sub>3</sub> is much more exothermic than the sorption of hydrogen in the metallic Pd (ca. - 20 kJ/mol H<sub>2</sub> during the formation of a diluted PdH phase).

Here, the samples of the physical mixture 2%Pd/MoO<sub>3</sub> + MoO<sub>3</sub> (1/1 by weight) is subjected to the hydrogen uptake experiment. In order to recognize easier the effect of added MoO<sub>3</sub>, the results obtained for the 2%Pd/MoO<sub>3</sub> + MoO<sub>3</sub> physical mixture are compared with previously obtained for the catalyst alone [33] (similar amounts ca. 0.2 g of both samples are used) (Fig. 8).

The amount of hydrogen sorbed in the process on Pd/MoO<sub>3</sub> + MoO<sub>3</sub> corresponds to the stoichiometry of hydrogen bronze H<sub>1.41</sub>MoO<sub>3</sub>. Its formation is accompanied by evolved heat of 102 kJ/mol H<sub>2</sub>. Thus, both samples show similar molar enthalpy of hydrogen sorption, namely -97 kJ/mol H<sub>2</sub> and -102 kJ/mol H<sub>2</sub> for the catalyst alone and the mixture of catalyst with MoO<sub>3</sub>, respectively.

However, some differences can be observed in the course of hydrogen uptake process. In both systems the rates of heat evolution are clearly increasing with the progress of saturation with hydrogen reaching pronounced maxima of heat evolution rate. Integration of the hydrogen uptake curves reveals, that those maxima correspond to hydrogen contents of H<sub>1.2</sub>MoO<sub>3</sub> and H<sub>0.97</sub>MoO<sub>3</sub> for the catalyst alone and mixture of 2%Pd/MoO<sub>3</sub> + MoO<sub>3</sub>, respectively. Further uptake of hydrogen generating bronzes of higher hydrogen content ( $x > 1 - 1.2$ ) is assisted by slowly decreases rate of heat evolution. This effect seems to be interesting however; further experiments are required to discuss it.

It is clear from these results, that the MoO<sub>3</sub> takes part in the bronze formation in the catalyst as well as when Pd/MoO<sub>3</sub> is physically mixed with the MoO<sub>3</sub>. Hence the hydrogen spill-over process, which, no doubts, is responsible for the bronze formation in the MoO<sub>3</sub>-supported catalysts must also operate between the MoO<sub>3</sub> grains. Thus, both components of the 2%Pd/MoO<sub>3</sub> + MoO<sub>3</sub> physical mixture are capable to hydrogen sorption during the hydrogen activation prior to the catalytic tests. Both could be therefore capable of incorporation of hydrogen into the reactants molecules. These microcalorimetric results could be useful in explaining observations from the catalytic tests.

In conclusion, activity and selectivity pattern of CAL hydrogenation on Pd/MoO<sub>3</sub> catalysts is observed to be determined by the Pd-loading in the catalysts. The Pd particles in all Pd/MoO<sub>3</sub> catalysts are within similar range, 8 – 10 nm in size. However, the extent of Pd particles aggregation gradually increases with growing Pd loading. As a result, specific activity presenting the rate of CAL hydrogenation normalized to the Pd mass is the highest on 0.5%Pd/MoO<sub>3</sub>, decreases with growing Pd loading up to 2%Pd/MoO<sub>3</sub> and then it stabilizes. It is also observed that irrespective of Pd-loading (0.5 to 4 wt % Pd), the selectivity to C=O hydrogenation on all Pd/MoO<sub>3</sub> catalysts is higher than that on inert support-containing Pd/SiO<sub>2</sub> catalyst. Such C=O selectivity promotion on Pd/MoO<sub>3</sub> catalysts could be related to the SMSI effect, similarly to what was reported for acrolein hydrogenation on 0.1%Pt/MoO<sub>3</sub> catalyst [21]. This effect has been related to electron-deficient sites created as a result of an association of metal atoms and electron-deficient cations on the molybdena surface generated upon high temperature hydrogen treatment [21]. The formation of these sites in the present Pd/MoO<sub>3</sub> catalysts (hydrogen treated at 250<sup>0</sup>C) could be evidenced by the XPS Pd 3d spectra (Fig. S 3). These sites may be expected to be related to the MoO<sub>3</sub> oxide/palladium interface. It should be stressed that the presence of aggregated Pd particles especially at high Pd-loading (4%Pd/MoO<sub>3</sub>) lowers the contribution of oxide/metal interface which could reduce selectivity effect induced by these interactions. Consequently, the C=O promotion selectivity on 4%Pd/MoO<sub>3</sub> is only slightly better than that on inert support-containing Pd/SiO<sub>2</sub> catalyst (Fig. 4 b).

However, in the present MoO<sub>3</sub> - supported catalysts an optimum Pd loading exists giving the best C=O selectivity, corresponding to 1%wt Pd-containing catalyst. The catalysts with either lower or higher Pd-loading promote the C=C hydrogenation. Moreover, a further promotion of C=C selectivity is attained on using physically mixed Pd/MoO<sub>3</sub> + MoO<sub>3</sub>. The promotion of C=C selectivity is then assisted by higher rate of CAL hydrogenation. Such improvement in performance induced by added MoO<sub>3</sub> was almost the same, irrespective of the Pd-loading in the 2%Pd/MoO<sub>3</sub> and 4%Pd/MoO<sub>3</sub> catalysts.

It has been already well documented that hydrogen bronze (H<sub>1.6</sub>MoO<sub>3</sub>) formed in the Pt/MoO<sub>3</sub> catalyst worked as hydrogen reservoir for the ethylene hydrogenation [19] as the formation of ethane proceeded due to the hydrogen arising from the bronze. In these catalysts, the Pt particles played a double role; they are the gates by which the H atoms may leave the host lattice and Pt acted as the catalytic sites [19]. Recent DFT calculations revealed that hydrogen molybdenum bronze itself can be a catalyst for hydrogenation of ethylene because the hydrogen on oxygen sites (Mo-O-H) of the bronze may activate ethylene via interaction with  $\pi$  electrons of ethylene [10]. An activation of ethylene on the hydrogen bronzes was calculated to be weak and resulted in a one-step C=C hydrogenation reaction in contrast to two-step process on transition metals surface characterized by strong ethylene chemisorption. A weak adsorption on the hydrogen bronzes makes the ethylene molecule susceptible for attack from the nearby hydrogen-species only. Consequently, the hydrogenation of unsaturated C=C of ethylene to give ethane becomes the only reactive route

available on the hydrogen bronzes surface [10]. For hydrogen bronzes catalyzed ethylene hydrogenation activation energy comparable to or smaller than the activation energy on the Pt-catalyst was calculated.

A higher rate of CAL hydrogenation assisted by promotion of the C=C hydrogenation on the Pd/MoO<sub>3</sub> + MoO<sub>3</sub> physical mixture may be therefore related to reactivity of hydrogen bronzes. It seems reasonable to assume that in CAL hydrogenation on Pd/MoO<sub>3</sub> catalysts apart from the Pd-sites also hydrogen bronzes may participate providing some additional sites and/or hydrogen species for the reaction. A remarkable promotion of the C=C hydrogenation in the CAL is then observed. It is well known that hydrogenation of C=C bond is thermodynamically preferred over that of C=O in the unsaturated aldehydes [22]. It seems that selectivity behavior of the Pd/MoO<sub>3</sub> catalysts with higher Pd-loading is mostly determined by the palladium reactivity. On the other hand, at low Pd-loading e.g. when a role of oxide/metal interface is weak an effect of hydrogen bronzes participation manifest more distinctly.

Hence, catalytic results obtained in CAL hydrogenation clearly show a vital role of hydrogen bronzes in the activity/selectivity pattern obtained using MoO<sub>3</sub> - supported Pd catalysts. The hydrogen bronzes could be not only reservoirs for hydrogen species but they may also promote the C=C hydrogenation of CAL yielding saturated aldehyde (HCAL). The obtained results also demonstrate that hydrogen species in the bronzes structure could have a beneficial effect on the palladium crystallites formation upon reduction of palladium ions -containing MoO<sub>3</sub>, a precursor of final catalyst. Besides commonly observed the Pd crystallites of spherical shapes, the Pd nanocrystals of well developed tetrahedral shape are also formed in the Pd/MoO<sub>3</sub> catalysts (Fig. 3). High mobility of hydrogen species in the bronzes structure assisted by easy migration of palladium ions facilitated by layered morphology of MoO<sub>3</sub> could promote the Pd crystallites of tetrahedral shape formation. This effect may also be responsible for specific location of Pd-particles in the oxide matrix in form of a well organized structures consisting of parallel chains of palladium particles (Fig. 2).

#### 4. Conclusions

The catalytic properties of Pd/MoO<sub>3</sub> of Pd content (0.5 – 4 wt %) are compared with that of Pd/SiO<sub>2</sub> a reference catalyst, known to be “inert” support. Additional information on the interaction of Pd/MoO<sub>3</sub> catalysts with hydrogen are provided by the microcalorimetric experiments. The impregnation of MoO<sub>3</sub> support with palladium acetate followed by hydrogen reduction (250<sup>0</sup>C) produces Pd/MoO<sub>3</sub> catalysts of Pd particles ca. 8-10 nm, regardless of the metal loading. Besides dominating spherically shaped and nearly monodispersed Pd particles, also some tetrahedral Pd crystallites appeared. High mobility of hydrogen species in the bronzes structure assisted by easy migration of palladium ions facilitated by layered morphology of MoO<sub>3</sub> accompanied by structural changes during the reduction could promote the Pd crystallites of tetrahedral shape. This effect may be also responsible for specific location of Pd-particles in the oxide matrix in the form of well organized

structures. A fraction of the particles form parallel arrangements located along the edges of the plates. The Pd particles are well distributed at low Pd-loading, 0.5 %Pd/MoO<sub>3</sub>. As the content of Pd increases the agglomeration of Pd nanoparticles grows. All the Pd/MoO<sub>3</sub> catalysts display higher selectivity to C=O hydrogenation compared to Pd/SiO<sub>2</sub> catalyst. The content of Pd has an impact on activity and selectivity of Pd/MoO<sub>3</sub> catalysts. The activity of Pd/MoO<sub>3</sub> normalized to the Pd mass decreases with growing Pd-content in molybdena oxide. The C=C group of cinnamaldehyde was preferentially hydrogenated compared to the carbonyl (C=O) group on the Pd/MoO<sub>3</sub> catalysts with low (0.5 %Pd) and high (4%Pd) Pd contents indicating the effect of optimum Pd-loading in the selectivity of CAL hydrogenation. The activity/selectivity behavior of Pd/MoO<sub>3</sub> catalysts are related to an effect of hydrogen bronzes existing during the catalytic tests. The hydrogen bronzes could provide additional active sites efficient for activation of CAL assisted by promotion of C=C hydrogenation.

### **Acknowledgements**

This work was partially supported by the National Science Centre, Poland; grant no. 2012/07/B/ST4/00518. We are grateful to Dr. hab. Lidia Lityńska-Dobrzyńska for taking HRTEM images.

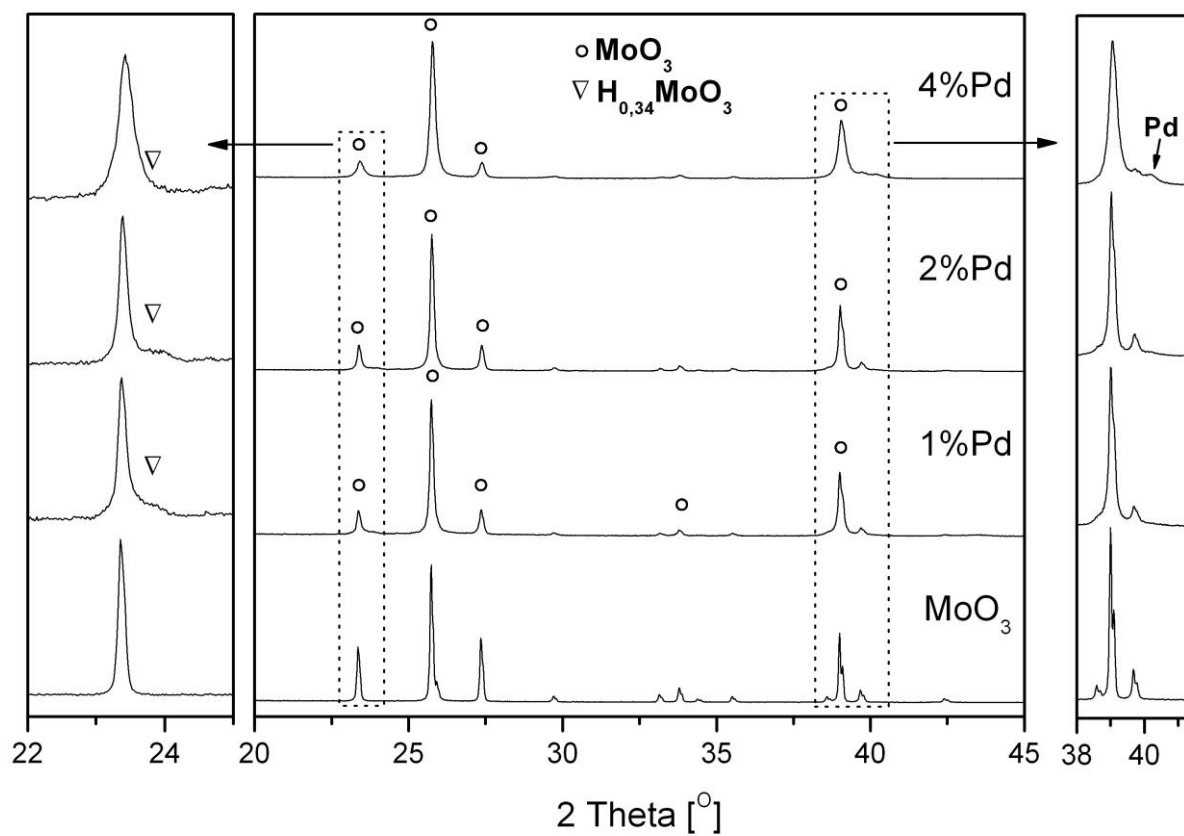
**References**

- [1] P. A. Sermon, G. C. Bond, *J. Chem. Soc. Faraday Trans. I*, 72 (1976) 730 – 744
- [2] T. Ressler, J. Wienold, R. E. Jentof, *Solid State Ionics*, 141-142 (2001) 243-251
- [3] S. Adams *J. Solid State Chem.*, 149 (2000) 75-87
- [4] K. M. Sancier, *J. Catal.* 23 (1971) 298,
- [5] X. Sha, L. Chen, A. C. Cooper, G. P. Pez, H. Cheng, *J. Phys. Chem. C* 113 (2009) 11399-11407
- [6] H. Noh, D. Wang, S. Luo, T. B. Flanagan, R. Balasubramanian, Y. Sakamoto *J. Phys. Chem. B* 108 (2004) 310-319
- [7] R. L. Smith, G. S. Rohrer *J. Catal* 163 (1996) 12-17;
- [8] L. Chen, A.C. Cooper, G. P. Pez, H. Cheng, *J. Phys. Chem. C* 112 (2008) 1755-1758
- [9] B. Li, W-L Yim, Q. Zhang, L. Chen, *J. Phys. Chem. C* 114 (2010) 3052-3058.
- [10] M. Yang, B. Han, H. Cheng, *J. Phys. Chem. C* 116 (2012) 24630-24638.
- [11] T. Matsuda, F. Uchijima, H. Sakagami, N. Takahashi, *Phys. Chem. Chem. Phys.*, 3 (2001) 4430-4436.
- [12] S. Al-Kandari, H. Al-Kandari, A. M. Mohamed, F. Al-Kharafi, A. Katrib, *Appl. Catal. A* 475 (2014) 497-502
- [13] H. Al-Kandari, A. M. Mohamed, S. Al-Kandari F. Al-Kharafi, G. A. Mekhemer, M. I. Zaki, A. Katrib, *J. Mol. Catal. A* 368-369 (2013) 1 - 8
- [14] T. Matsuda, H. Shiro, H. Sakagami, N. Takahashi, *Catal. Lett.*, 47 (1997) 99;
- [15] T. Matsuda, H. Shiro, H. Sakagami, N. Takahashi, *Appl. Catal. A* 193 (2000) 185;
- [16] J. Guan, G. Peng, Q. Cao, X. Mu, *J. Phys. Chem. C* 118 (2014) 25555-25566
- [17] P. A. Sermon, G.C. Bond *Catal. Rev. Sci. Eng* 8 (1973) 211,
- [18] P. A. Sermon, G.C. Bond *Trans. Faraday Soc.* 76 (1980) 889,
- [19] J. P. Marcq, X. Wispeninkx, G. Poncelet, D. Keravis, J. J. Fripiat, *J. Catal.* 73 (1982) 309-328
- [20] P.A. Zosimova, A. V. Smirnov, S. N. Nesterenko, V. V. Yuschenko, W. Sinkler, J. Kocal, J. Holmgren, I. I. Ivanova, *J. Phys. Chem. C* 111 (2007) 14790
- [21] C. Hoang-Van, O. Zegaoui *Appl. Catal. A* 164 (1997) 91-103
- [22] P. Gallezot, D. Richard, *Catal. Rev. Sci. Eng.*, 40 (1998) 81-126
- [23] F. Delbecq, P. Sautet, *J. Catal.* 152 (1995) 217-236.
- [24] F. Delbecq, P. Sautet, *J. Catal.* 211 (2002) 398-406.
- [25] P. Maki-Arvela, J. Hajek, T. Salmi, D. Yu. Murzin, *Appl. Catal. A* 292 (2005) 1-49.
- [26] D. Richard, J. Ockelford, A. Giroir-Fendler, P. Gallezot, *Catal. Lett.* 3 (1989) 53.
- [27], M. A. Pereira da Silva, R. A. Mello-Vieira, M. Schmal, *Appl. Catal. A* 190 (2000) 177;
- [28] S. D. Jackson, J. Willis, G. D. McLellan, G. Webb, M.B. T. Keegan, R. B. Moyes, S. Simpson, P. B. Wells, R. Whyman, *J. Catal.*, 139 (1993) 191
- [29] R. M. Navarro, B. Pawelec, J. M. Trejo, R. Mariscal, J. L. G. Fierro, *J. Catal.* 189 (2000) 184.
- [30] R. Kosydar, M. Góral, J. Gurgul, A. Drelinkiewicz, *Catal. Comm.* 22 (2012) 58-67

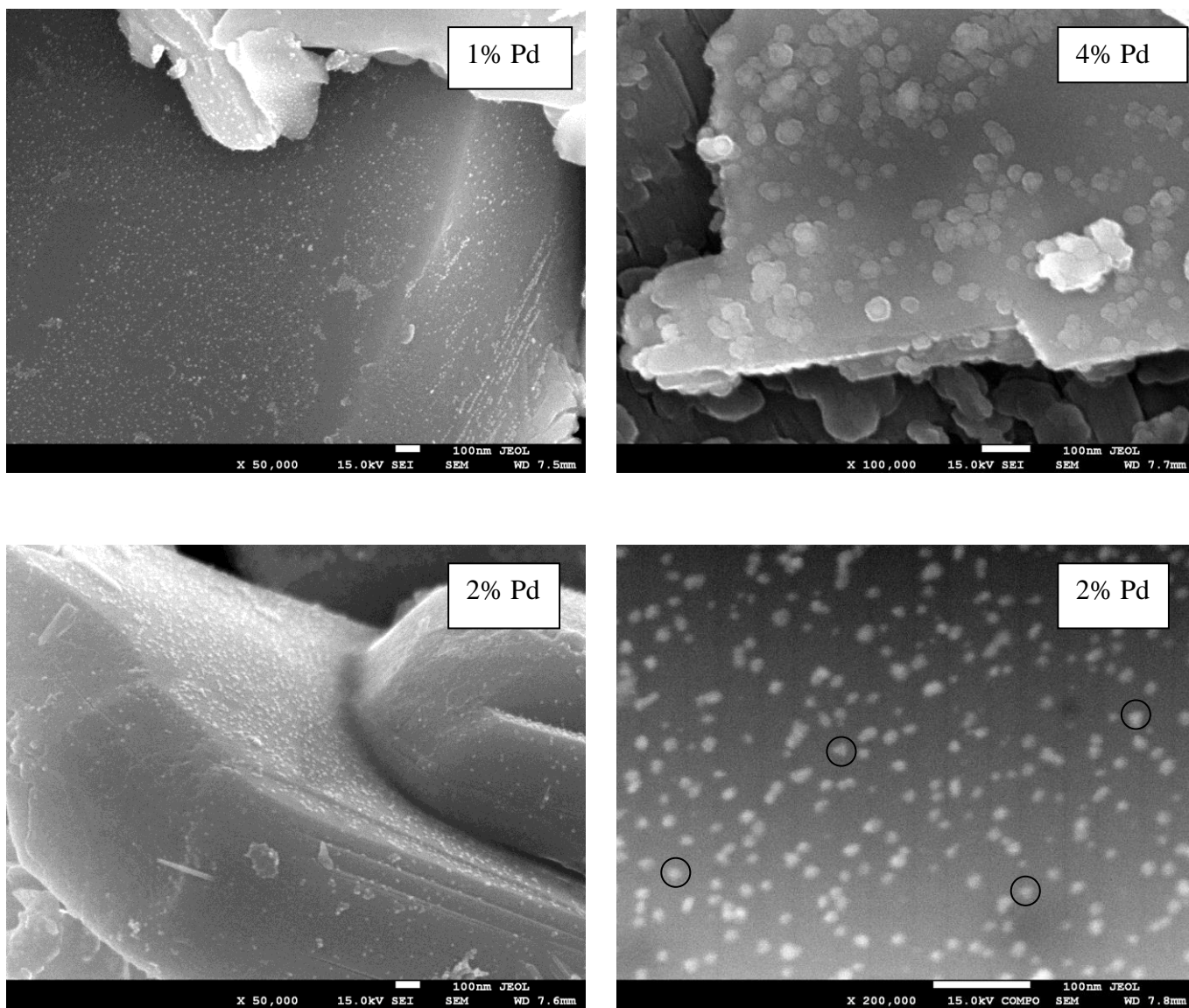
- [31] E. Lalik, R. Mirek, J. Rakoczy, A. Groszek, *Catal. Today*, 114 (2006) 242-247
- [32] A. Groszek, E. Lalik, J. Haber, *App. Surf. Sci.*, 256 (2010) 5498-5502
- [33] E. Lalik, M. Kołodziej, R. Kosydar, T. Szumelda, A. Drelinkiewicz, *Recycl. Catal.* 2 (2015) 27-35
- [34] T. Szumelda, A. Drelinkiewicz, R. Kosydar, J. Gurgul *Appl. Catal. A* 487 (2014) 1-15
- [35] M. Boutonnet, S. Logdberg, E. E. Svensson, *Current Opin. Colloid & Interface Sci.*, 13 (2008) 270-286
- [36] S. Erikson, U. Nylen, S. Rojas, M. Boutonnet, *Appl. Catal. A*, 265 (2004) 207-219,
- [37] E. Lalik, R. Kosydar, R. Tokarz-Sobieraj, M. Witko, T. Szumelda, M. Kołodziej, W. Rojek, T. Machej, E. Bielanska, A. Drelinkiewicz *Appl. Catal. A* 501 (2015) 27-40
- [38] F. Uchijima, T. Takagi, H. Itoh, T. Matsuda, N. Takahashi, *Phys. Chem. Chem. Phys.*, 2 (2000) 1077-1083.
- [39] C. Hoang-Van, O. Zegaoui *Appl. Catal. A* 130 (1995) 89-103
- [40] M. Susic, Y. Solonin *J. Mater. Sci.*, 24 (1989) 3691-3698
- [41] T. Matsuda, F. Uchijima, S. Endo, N. Takahashi, *Appl. Catal. A* 176 (1999) 91-99
- [42] G. Bond, J. B. P. Tripathi, *J. Chem. Soc. Faraday Trans. 1* 72 (1976) 933-041
- [43] P. G. Dickens, J. J. Birtill, C. J. Wright, *J. Solid State Chem.*, 28 (1979) 185
- [44] J. J. Birtill, P. G. Dickens *Mat. Res. Bull.*, 13 (1978) 311-316
- [45] N. Sotani, K. Eda, M. Kunitomo *J. Chem. Soc. Farady Trans. 86* (1990) 1583-1586
- [46] Y. Wang, S. Xie, J. Liu, J. Park, Ch. Z. Huang, Y. Xia, *Nano Letters* 13 (2013) 2276-2281
- [47] H. Zhu, Q. Chi, Y. Zhao, Ch. Li, H. Tang, J. Li, T. Huang, H. Liu *Mater. Res. Bull.*, 47 (2012) 3637-3643
- [48] R.I. Declerck-Grimee, P. Canesson, R. M. Friedman, J. J. Fripiat, *J. Phys. Chem.*, 82 (1978) 885;
- [49] A. Cimino, B. de Angelis *J. Catal.*, 36 (1975) 11.
- [50] W. Grunert, A. Yu. Stakheev, R. Feldhaus, K. Anders, E. S. Shpiro, K. M. Minachev, *J. Phys. Chem.* 95 (1991) 1323-1328.
- [51] A. Hammoudeh, S. Mahmoud *J. Mol. Catal. A*: 203 (2003) 231-239.
- [52] S. Mahmoud, A. Hammoudeh, S. Gharaibeh, J. Melsheimer, *J. Mol. Catal. A*; 178 (2002) 161
- [53] G. R. Cairns, R. J. Cross, D. Stirling *J. Catal.* 166 (1997) 89-97.
- [54] A. Cabiacc, T. Cacciaguerra, P. Trens, R. Durand, G. Delahay, A. Medevielle, D. Plee, B. Coq, *Appl. Catal. A* 340 (2008) 229-235
- [55] T. Matsuda, S. Uozumi, N. Takahashi, *Phys. Chem. Chem. Phys* 6 (2004) 665-672.
- [56] H. Yamada, H. Urano, S. Goto, *Chem. Eng. Sci.*, 54 (1999) 5231-5235,
- [57] L. Zhang, J. M. Winterbottom, A. P. Boyes, S. Raymahasay, *J. Chem. Technol. Biotechnol.* 72 (1998) 264-272
- [58] X. Yang, D. Chen, S. Liao, H. Song, Y. Li, Z. Fu, Y. Su, *J. Catal.* 291 (2012) 36-43
- [59] A. C. Krauth, G. H. Bernstein, E. E. Wolf, *Catal. Lett.* 45 (1997) 177-186

- [60] X. Xie, Y. Li, Z-q. Liu, M. Haruta, W. Shen, *Nature Letters*, 458 (2009) 746-749
- [61] R. Liu, Y. Yu, K. Yoshida, G. Li, H. Jiang, M. Zhang, F. Zhao, S-I. Fujita, M. Arai, *J. Catal.* 269 (2010) 191-200
- [62] H. Noh, D. Wang, S. Luo, T. B. Flanagan, Y. Sakamoto, *J. Phys. Chem. B*, 108 (2004) 310-319
- [63] S. Triwahyono, A. A. Jalil, S. N. Timmiati, N. N. Ruslan, H. Hattori, *Appl. Catal. A*, 372 (2010) 103 – 107.

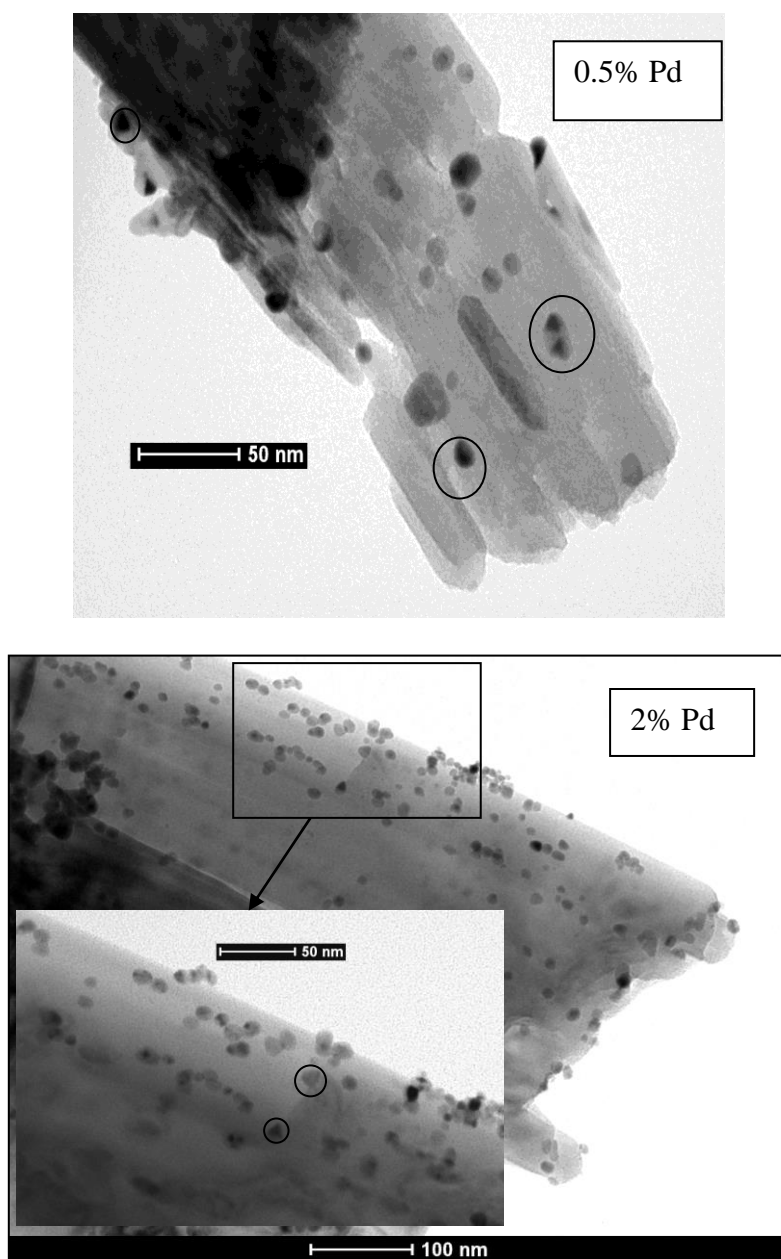
## List of Figures



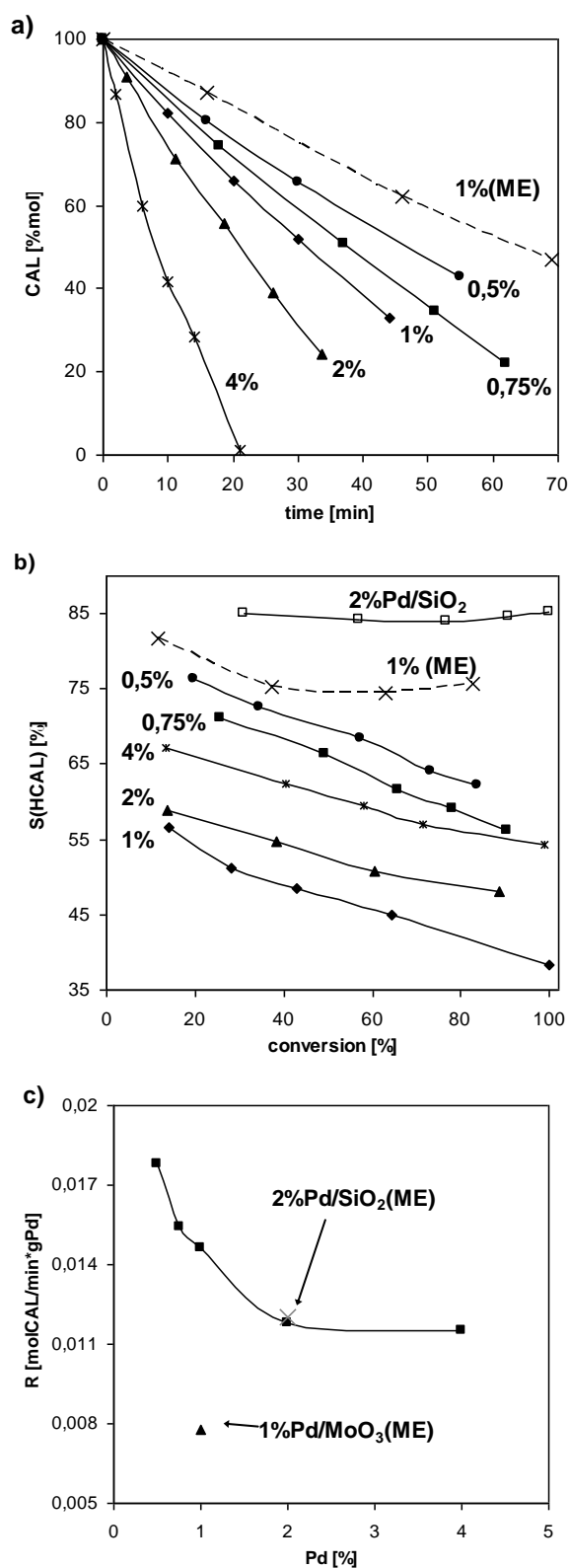
**Fig. 1.** XRD diffraction pattern of Pd/MoO<sub>3</sub> catalysts prepared by impregnation method and reduced with hydrogen at 250°C



**Fig. 2.** SEM images of 1%Pd/MoO<sub>3</sub>, 2%Pd/MoO<sub>3</sub> and 4%Pd/MoO<sub>3</sub> catalysts synthesized by impregnation method followed by hydrogen reduction

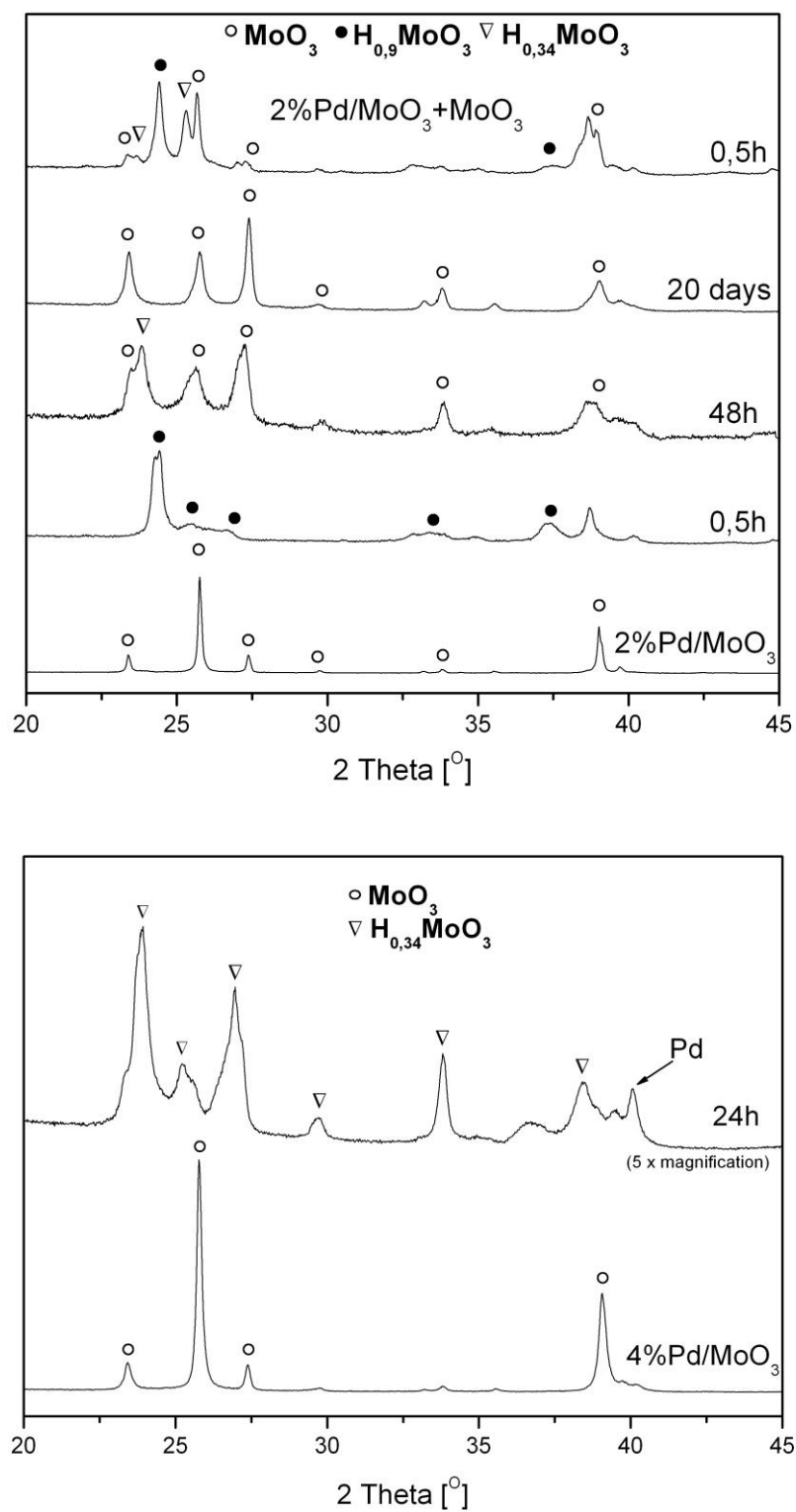


**Fig. 3.** TEM and HRTEM images of 0.5%Pd/MoO<sub>3</sub> and 2%Pd/MoO<sub>3</sub> catalysts synthesized by impregnation method followed by hydrogen reduction

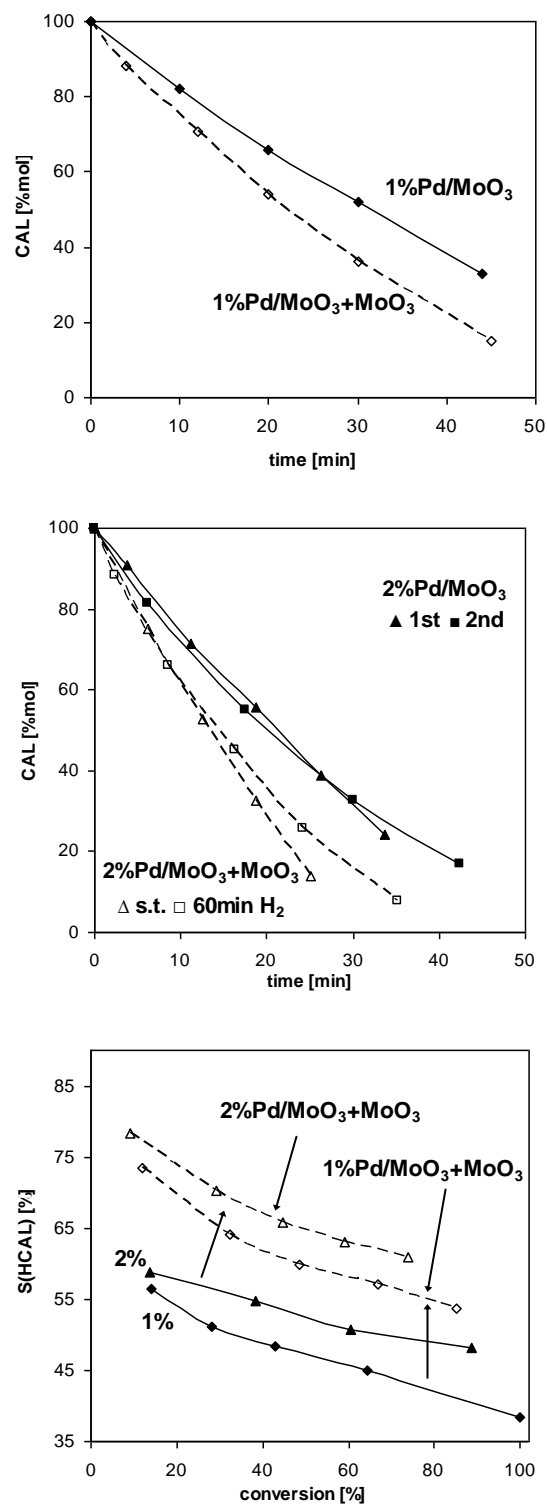


**Fig. 4.** Hydrogenation of CAL on Pd/MoO<sub>3</sub> catalysts of various Pd-loading. The decrease of CAL concentration (a), selectivity to saturated aldehyde (HCAL) (b) and Initial rate of CAL hydrogenation normalized to the Pd mass against Pd-loading in the Pd/MoO<sub>3</sub> catalysts (c)

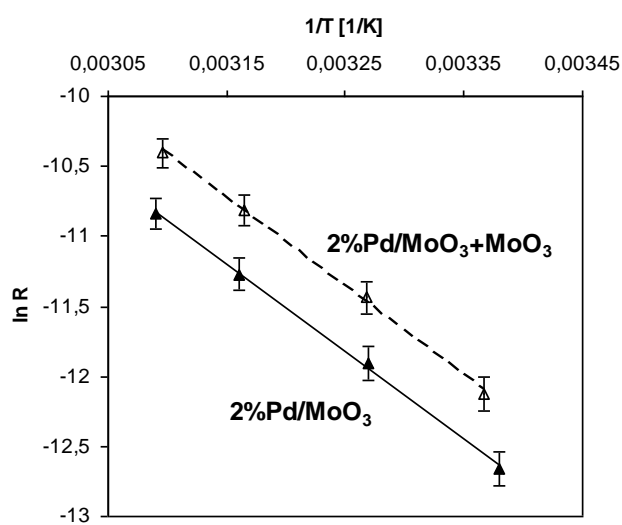
Reaction conditions: toluene, temperature 50°C, catalyst concentration 5 g/dm<sup>3</sup>, CAL concentration 0.05 mol/dm<sup>3</sup>



**Fig. 5.** XRD diffraction patterns of recovered 2%Pd/MoO<sub>3</sub> and 4%Pd/MoO<sub>3</sub> catalysts

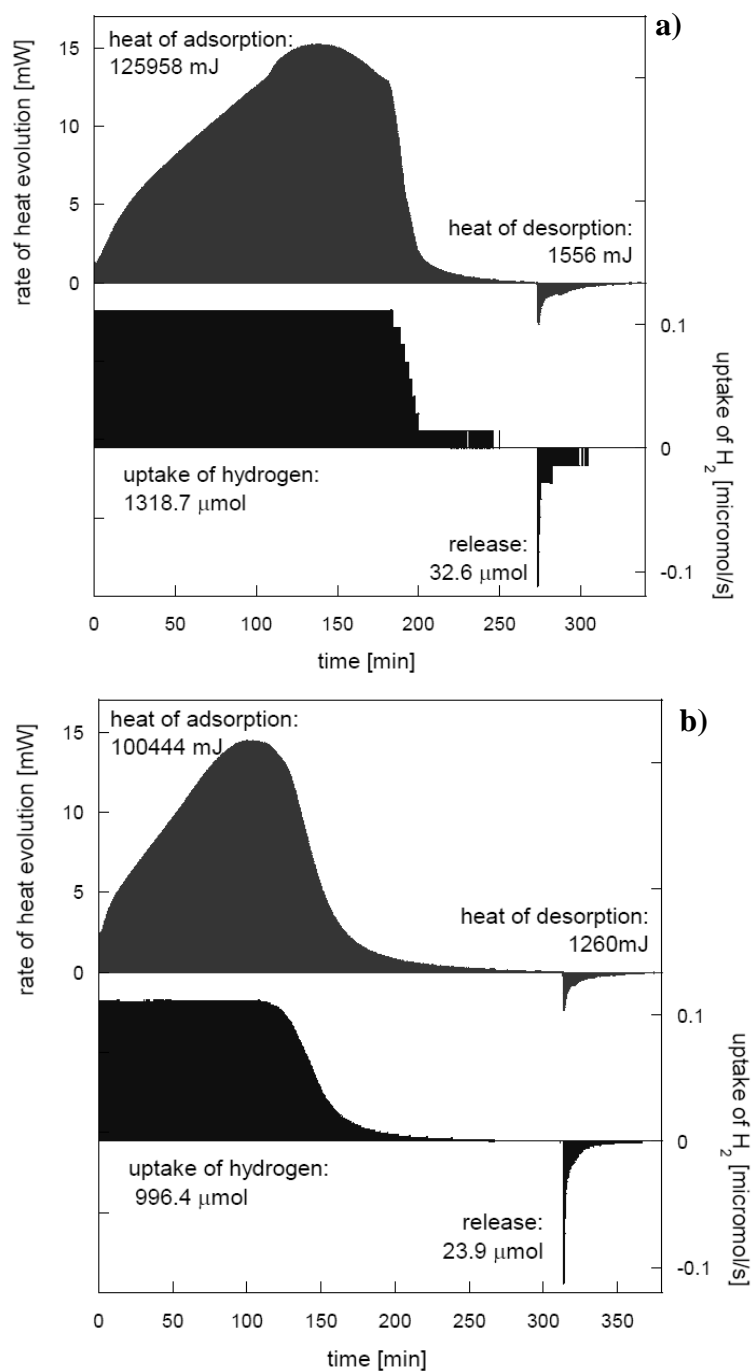


**Fig. 6.** Hydrogenation of CAL on physically mixed Pd/MoO<sub>3</sub> + MoO<sub>3</sub> catalysts. The decrease of CAL concentration and the selectivity to saturated aldehyde (HCAL)  
Reaction conditions: see Fig. 4

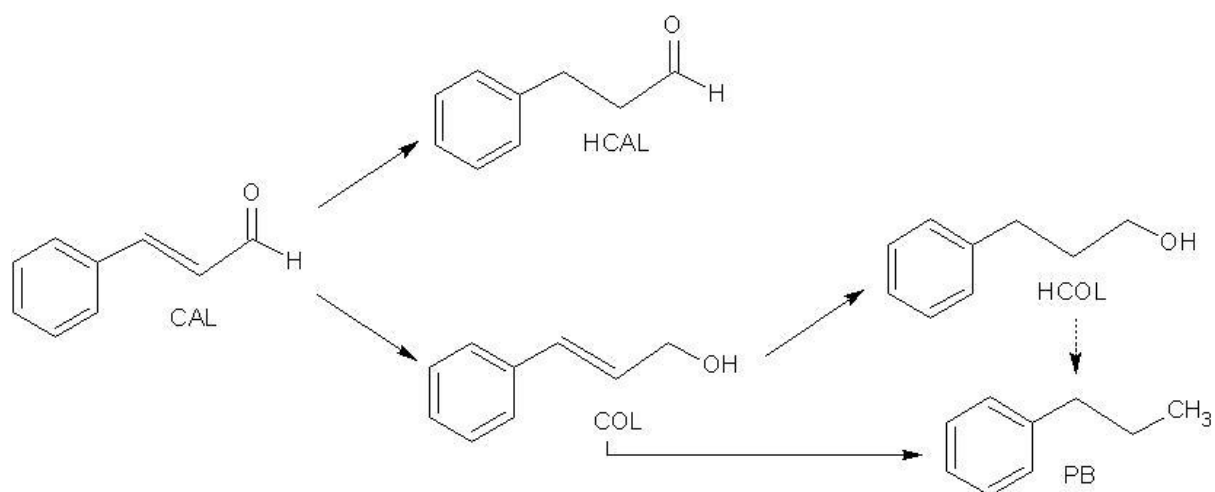


**Fig. 7.** Arrhenius plots obtained for CAL hydrogenation on 2%Pd/MoO<sub>3</sub> and 2%Pd/MoO<sub>3</sub> + MoO<sub>3</sub> samples.

Reaction conditions: toluene, temperature 23 - 50°C, catalyst concentration 5 g/dm<sup>3</sup>, CAL concentration 0.05 mol/ dm<sup>3</sup>



**Fig. 8.** The microcalorimetric experiments of hydrogen uptake by 2%Pd-Pt/MoO<sub>3</sub> (a) and physical mixture 2%Pd/MoO<sub>3</sub> + MoO<sub>3</sub> (b). The rate of heat evolution (upper curves) and the rate of hydrogen uptake (bottom curves) against the time of experiment duration. Experimental conditions: temperature of 22<sup>0</sup>C, atmospheric pressure, 5% H<sub>2</sub> in N<sub>2</sub>, flow rate 3 cm<sup>3</sup>/min.

**Scheme 1**

Reaction pathways of cinnamaldehyde hydrogenation